Self-organization of quantum dots in epitaxially strained solid films

A. A. Golovin and S. H. Davis
Department of Engineering Sciences and Applied Mathematics, Northwestern University, Evanston, Illinois 60208-3100, USA

P. W. Voorhees
Department of Materials Sciences, Northwestern University, Evanston, Illinos 60208-3100, USA
(Received 11 December 2002; published 3 November 2003)

A nonlinear evolution equation for surface-diffusion-driven Asaro-Tiller-Grinfeld instability of an epitaxially strained thin solid film on a solid substrate is derived in the case where the film wets the substrate. It is found that the presence of a weak wetting interaction between the film and the substrate can substantially retard the instability and modify its spectrum in such a way that the formation of spatially regular arrays of islands or pits on the film surface becomes possible. It is shown that the self-organization dynamics is significantly affected by the presence of the Goldstone mode associated with the conservation of mass.

DOI: 10.1103/PhysRevE.68.056203 PACS number(s): 68.65.Hb, 68.55.−a, 89.75.Kd

I. INTRODUCTION

Spontaneous formation of nanoscale islands (quantum dots) on surfaces of epitaxially strained thin solid films is a potentially efficient route to producing large arrays of dots required for a new generation of electronic devices. These islands form by a Stranski-Krastanow growth process whereby the planar film surface undergoes a morphological instability of Asaro-Tiller-Grinfeld type [1]. The instability is driven by the stress created by the lattice parameter mismatch between the film and substrate and results in the formation of dislocation-free islands [2]. After formation, the islands can coarsen, with larger islands growing at the expense of the smaller ones [3], or evolve into a system of islands with almost uniform sizes [4]. While significant insights into the conditions governing the coarsening of islands have been made by considering the energetics of island formation [5], the *dynamics* of island formation has received much less attention. Fully dynamical descriptions of stress-driven island formation during heteroepitaxy have usually been limited to numerical simulations of the evolution of small numbers of three-dimensional islands [6], though one recent work [7] explores a large number of dots in three dimensions by means of large-scale three-dimensional computer simulations.

Another promising route to studying the dynamics of the formation of large numbers of dots is to derive an evolution equation for the film surface shape, $h(\mathbf{r},t)$. This approach delivers greater insight into the mechanism of the dot formation and evolution at much lower cost. A simple (dimensionless) evolution equation that captures much of the relevant physics can be derived in the limit of a perfectly rigid substrate, in a small-slope approximation near the instability threshold [8]

$$\partial_t h = \nabla^4 h + \beta \nabla^6 h + \nabla^2 \left[h \nabla^2 h + \frac{1}{2} |\nabla h|^2 \right], \qquad (1)$$

where $\mathbf{r}=(x,y)$ are coordinates along the planar surface, and β is the coefficient depending on the Poisson ratio of the film. Generalization of Eq. (1) for the case of an infinitely deep, elastic substrate has been performed recently in Ref. [9]. In both cases, the solutions blow up in finite times, similar to the boundary-integral computations for semifinite stressed solids that exhibit formation of a cusplike surface morphology with the speed of the cusp tip approaching infinity [10]. Examples of the blow-up solutions of Eq. (1) are shown in Fig. 1.

One can argue that these evolution equations can describe the tendency towards the formation of islands. However, it is desirable to have a model describing the *saturation* of the instability and the formation of *finite-size structures* as observed in experiments. In this paper, we show that a possible mechanism for the formation of uniform-size quantum dots and even spatially regular arrays of islands is the *wetting interaction* between the film and the substrate. We demonstrate, within the framework of a small-slope approximation, that this interaction changes the instability spectrum so that the instability at onset can correspond to perturbations with a small but nonzero wave number. This makes the formation of spatially periodic patterns possible. We show that certain wetting potentials between the film and the substrate can lead to a nonlinear stabilization of the instability near threshold, and to the self-organization of spatially regular arrays of either quantum dots or nanopits.

II. EVOLUTION EQUATION IN THE PRESENCE OF WETTING INTERACTIONS

Consider an epitaxially strained thin solid film that wets a perfectly rigid solid substrate. The shape of the film surface evolves due to surface diffusion to decrease the elastic energy of the film. This evolution is described by the following equation [8]:

$$\frac{\partial_t h}{\sqrt{1+|\nabla h|^2}} = \mathcal{D}\nabla_S^2[\mathcal{E}(h) + \gamma \mathcal{K} + \Phi], \qquad (2)$$

where $\mathcal{D}$ is a constant proportional to the surface diffusivity, $\mathcal{E}(h)$ is the elastic energy density at the surface found from the solution of the elastic problem [2,8], γ is surface energy, $\mathcal{K}$ is the curvature of the surface, and $\Phi(h,|\nabla h|^2,\nabla^2 h)$ is a

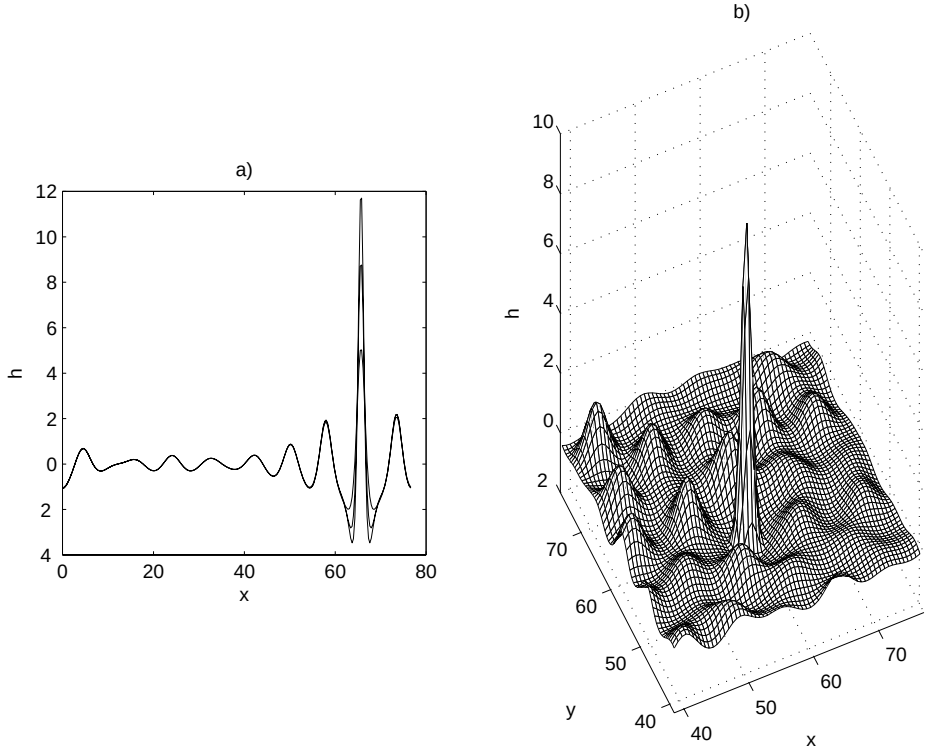

FIG. 1. Blow-up solutions of Eq. (1) in 1D (a) (different graphs corresponds to different moments of time) and in 2D (b) (at a particular moment of time).

wetting chemical potential that generally can be considered as a function of the film thickness, slope, and curvature. Such a general form encompasses models of the wetting layer which involve nonlinear elasticity [11] as well as height-dependent surface energy $\gamma=\gamma_s+(\gamma_f-\gamma_s)\Gamma(h)$, where $\gamma_{s,f}$ are surface energies of the substrate and the thick film, respectively, and $\Gamma(h)$ ranges from 0 to 1 when h varies from 0 to ∞ [12]. For example, in the latter case, $\Phi=\gamma(h)\mathcal{K}+(d\gamma/dh)/\sqrt{1+|\nabla h|^2}$. In the case of the van der Waals–type wetting interactions, $\Phi=A/h^n$. For some metals and semiconductors other forms of wetting potentials are possible. Also, a wetting potential can be anisotropic, it can depend on the orientation of the solid film free surface, i.e., on its slope. In the latter case, it can depend not only on the absolute value of the surface slope but also on its sign. However, for highly symmetric surface orientations only absolute value of the surface slope would matter.

Thus, the problem with the wetting solid film differs from that in Ref. [8] only by the addition of the functional $\Phi(h,|\nabla h|^2,\nabla^2 h)$. The small-slope analysis carried out in Ref. [8] for the case of a perfectly rigid substrate is easily repeated for this case to yield the following dimensionless evolution equation for the scaled surface shape H:

$$\partial_T H=\nabla^2\left\{(H-1)\nabla^2 H+\frac{1}{2}(\nabla H)^2+\frac{\mathcal{D}\tau}{\alpha^2 L^3}\Phi\left(LH,\alpha^2|\nabla H|^2,\frac{\alpha^2}{L}\nabla^2 H\right)\right\}+O(\alpha^2). \tag{3}$$

Here, according to Ref. [8], the spatial scale is $L=\gamma/(4\mu\delta^2)$ and the time scale is $\tau=L^3/(4\mu\delta^2\mathcal{D})$, where $\delta\ll 1$ is the lattice misfit of the epitaxially strained film, μ is the elastic shear modulus, $\alpha\ll 1$ is the slope parameter, and dimensionless space and time coordinates are long scale, i.e., $\nabla\sim\alpha,\partial_T\sim\alpha^2$. The terms $O(\alpha^2)$ in Eq. (3) are computed in Ref. [8].

First, we neglect the dependence of the wetting potential on the curvature of the film surface, thus considering $\Phi(h,|\nabla h|^2)$, and assume that

$$\left(\frac{\mathcal{D}\tau}{L^2}\right)\frac{\partial\Phi(L,0)}{\partial h}=\alpha^4 a,$$

$$\left(\frac{\mathcal{D}\tau}{L}\right)\frac{\partial^2\Phi(L,0)}{\partial h^2}=2\alpha^2 b, \tag{4}$$

$$\left(\frac{\mathcal{D}\tau}{L^3}\right)\frac{\partial\Phi(L,0)}{\partial|\nabla h|^2}=c,$$

where a, b, and c are $O(1)$ constants. Then, taking $H=1+\alpha^2[\eta+h(\mathbf{r},t)]$, $\eta=$const, and introducing a new time scale $t=\alpha^2 T$, one obtains, after appropriate rescaling, the following evolution equation for h:

$$\partial_t h=g\nabla^2 h+\nabla^4 h+\nabla^6 h+\nabla^2[h\nabla^2 h+p(\nabla h)^2+qh^2], \tag{5}$$

where

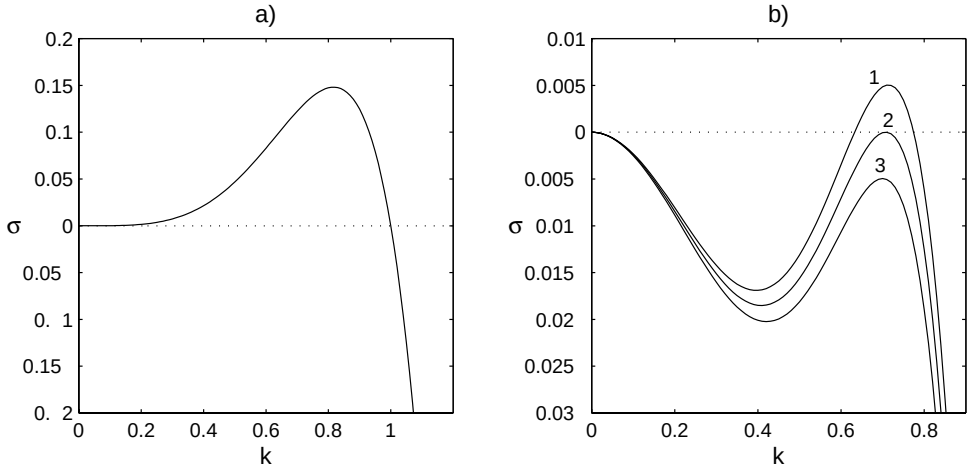

FIG. 2. Dispersion curves $\sigma(k)$ for the ATG instability of a solid film on a rigid substrate (a) without wetting interactions and (b) with wetting interactions: (1) $g<g_c$, (2) $g=g_c$, (3) $g>g_c$.

$$g=a\beta\eta^{-2},\quad p=\frac{1}{2}+c,\quad q=b\beta\eta^{-1},\quad \beta=\frac{3+4\nu}{6(1-\nu)}, \tag{6}$$

and ν is the Poisson ratio. The linear term with the sixth derivative comes from $O(\alpha^2)$ nonlinear terms in Eq. (3) after the rescaling (see Ref. [8] for details).

Equation (5) describes the nonlinear evolution of a thin, epitaxially strained film in the presence of wetting interactions with the substrate. One can see that wetting interactions suppress the instability (see also Refs. [13,11,14]) and change the spectrum of linear perturbations of the film surface $\sim e^{\sigma t+i\mathbf{k}\cdot\mathbf{r}}$ from $\sigma=k^4-k^6$ for Eq. (1) to $\sigma=-gk^2+k^4-k^6$, see Fig. 2. Thus, the instability occurs for $g<g_c=1/4$ at a wave number $k_c=\sqrt{2}/2$, which makes formation of stationary, spatially periodic patterns possible in this system.

III. PATTERN FORMATION IN 1+1 SYSTEM

First, we consider a 1+1 system [two-dimensional (2D) film with 1D surface] since some important features of the nonlinear evolution of the film instability can be studied in this case.

A. Weakly nonlinear analysis

In order to study the possibility of pattern formation we shall first perform a weakly nonlinear analysis of stationary solutions of Eq. (5) near the instability threshold. A characteristic feature of the system described by Eq. (5) is the presence of the Goldstone mode $\sigma=0$, corresponding to $k=0$ (see Fig. 2) and associated with the conservation of mass. The nonlinear interaction between the Goldstone mode and the unstable mode can substantially affect the system behavior near the instability threshold [15,16] and must be taken into account in weakly nonlinear analyses.

Consider a 1D version of Eq. (5). Take $g=g_c-2\epsilon^2$ and

$$h\sim\epsilon A(X,T)e^{ik_cx}+\text{c.c.}+\epsilon^2B(X,T)+\cdots,$$

where A is the complex amplitude of the unstable mode, B is the real amplitude of the Goldstone mode, $X=\epsilon x$, and $T=\epsilon^2 t$. Standard multiple-scale analysis near the bifurcation point yields the following system of equations for A and B:

$$\partial_T A=A+A_{XX}-\lambda_0|A|^2A+sAB, \tag{7}$$

$$\partial_T B=mB_{XX}+w(|A|^2)_{XX},$$

where

$$\lambda_0=\frac{2}{9}(1+p-2q)\left(p+q-\frac{5}{4}\right), \tag{8}$$

$$m=\frac{1}{4},\quad s=\frac{1}{4}-q,\quad w=-1+p+2q.$$

System (7) is similar to that obtained in Ref. [17] for the interaction between long- and short-scale modes of Marangoni convection in a thin liquid layer with a deformable interface. It can also be considered as a generic system describing nonlinear evolution in a large class of unstable systems with a conserved quantity [16,19].

For $\lambda_0>0$ the periodic structure is supercritical and can be stable, while for $\lambda_0<0$ it is subcritical and blows up in a finite time. The conclusion about stability of the supercritical pattern, however, cannot be made unless the interaction with the Goldstone mode is taken into account. For $\lambda_0>0$, stationary solution of the system (7),

$$A_0=\lambda_0^{-1/2},\quad B_0=0, \tag{9}$$

corresponds to a 1D periodic array of ''islands.'' Consider perturbations $\tilde{A},\tilde{B}$ of the solution (9) in the form

$$\tilde{A}=\tilde{a}e^{iQX+\omega T}+\tilde{b}e^{-iQX+\omega^*T},\quad \tilde{B}=\tilde{c}e^{iQX+\omega T}+\text{c.c.},$$

where ω^* is the complex conjugate of ω. One easily obtains from Eq. (7) that the stationary solution becomes unstable with respect to monotonic perturbations, $\text{Im}(\omega)=0$, for

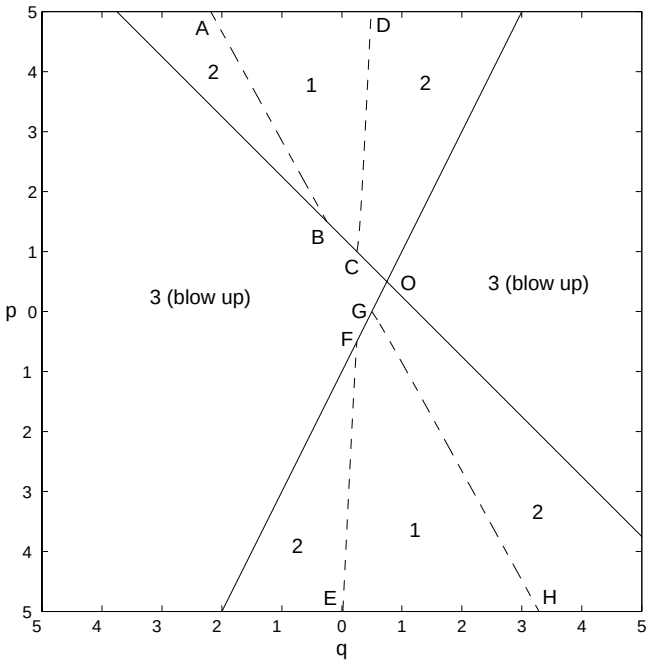

FIG. 3. Regions corresponding to different types of excitation and stability of spatially periodic 1D solutions of Eq. (5) near threshold: (1) supercritical stable; (2) supercritical unstable; (3) subcritical. Coordinates of the points are: $O(0.75,0.5)$, $B(-0.25,1.5)$, $C(0.25,1)$, $F(0.25,-0.5)$, and $G(0.5,0)$.

$$\frac{sw}{m}+\lambda_0<0. \tag{10}$$

Condition (10) allows one to determine regions in the (q,p) plane corresponding to different types of pattern excitation and stability near threshold, as shown in Fig. 3. The straight lines OCB and OGF correspond to $\lambda_0=0$ and the curves AB, CD, EF, and GH are parts of the hyperbola $sw/m+\lambda_0=0$. It is interesting that at the intersection point O, $p=1/2$ and $q=3/4$. Since $p=1/2$ corresponds to $c=0$, this means that unless the wetting potential depends on the film slope, the periodic structure is always subcritical and therefore blows up. Weakly nonlinear analysis is not useful in this case.

B. Numerical simulations

In order to study the evolution of the formation of 1D arrays of islands farther from the instability threshold, we have performed numerical simulations of Eq. (5) by means of a pseudospectral code with periodic boundary conditions. For the parameter values corresponding to region 1 in Fig. 3, near the instability threshold, one observes the formation of a sinusoidal surface profile. With the increase of the supercriticality (i.e., with the decrease of g from $g_c=1/4$), the surface shape becomes significantly nonharmonic and exhibits two typical periodic patterns: periodic arrays of ''cone''-type islands and ''cap''-type islands shown in Fig. 4. Cones and caps are observed for $p>0$ and $p<0$, respectively.

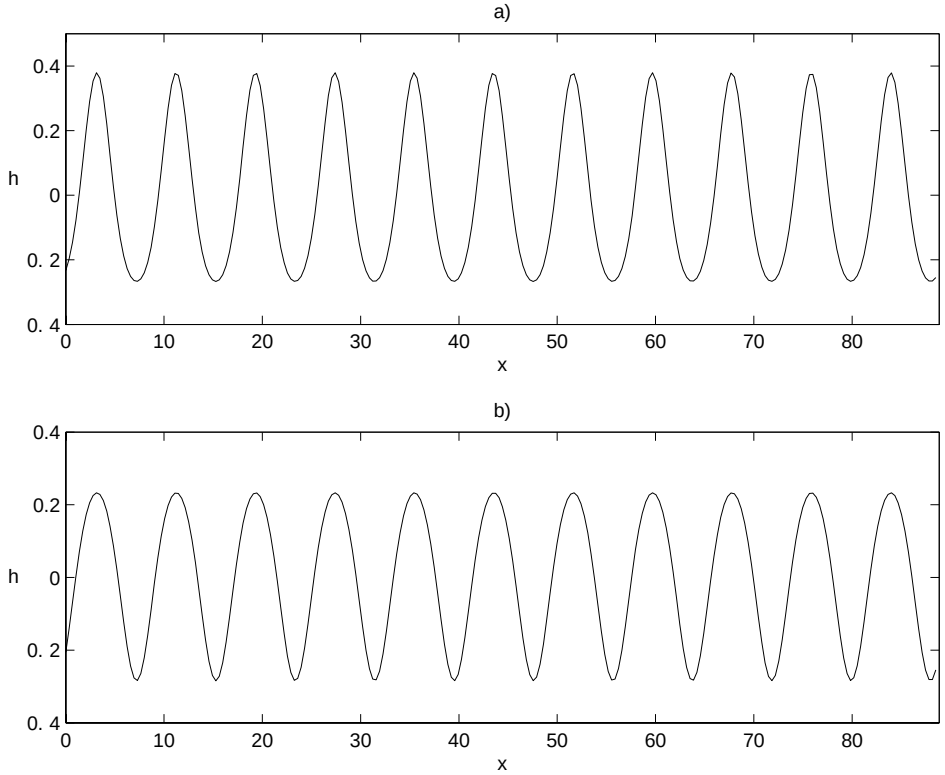

FIG. 4. Stationary numerical solutions of Eq. (5) in 1D for $(g,q,p)=$ (a) $(0.1,-1.0,4.0)$ (cones) and (b) $(0.1,1.0,-4.0)$ (caps).

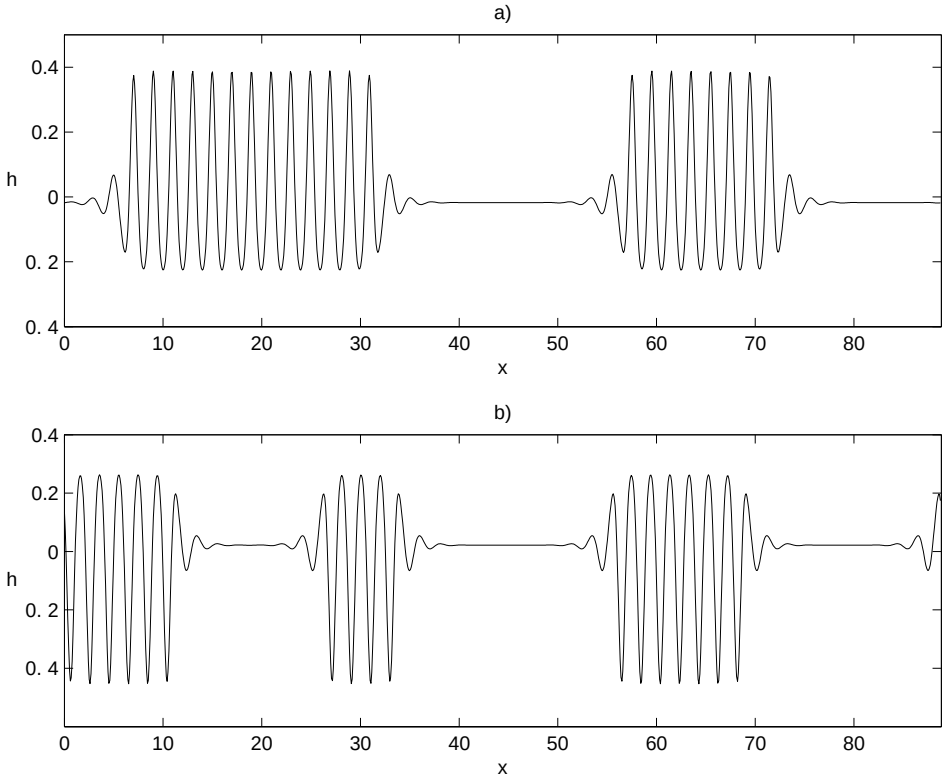

FIG. 5. Localized stationary solutions of Eq. (5) in 1D: (a) patches of cones, $g=0.24$, $p=4.0$, $q=-2.3$; (b) patches of caps, $g=0.248$, $p=-3.0$, $q=3.0$.

For the values of the parameters p and q from region 2 in Fig. 3, where periodic arrays of islands near the instability threshold are unstable due to the presence of the Goldstone mode, one observes the formation of localized (or strongly modulated) patches of islands shown in Fig. 5. Depending on the sign of the parameter p, these can be either patches of cones or caps. They correspond to stationary solutions of the system (7), $A(x)$ and $B(x)$, which are obtained in terms of Jacobi elliptic functions and analyzed in detail in Ref. [16].

Localized solutions shown in Fig. 5 are predicted only near the instability threshold in the region 2 in Fig. 3. With the increase of the supercriticality, one observes either the formation of periodic arrays of cones or caps, or the blow-up. The latter can be of either ''island'' type, similar to that exhibited by solutions of Eq. (1) without wetting interactions, shown in Fig. 1, or a ''pit'' type. These two types of the blow-up are shown in Fig. 6. Note that spontaneous formation of nanopits has been recently observed in experiments [21].

IV. PATTERN FORMATION IN 2+1 SYSTEM

More interesting is the $2+1$ case of a 3D film with a 2D surface whose evolution is described by Eq. (5). Note that Eq. (5) does not have the symmetry $h\rightarrow -h$. In this case, the instability whose threshold corresponds to a finite wave number (see Fig. 2) usually results in a hexagonal pattern that occurs via a transcritical bifurcation [20,22]. In this section we concentrate on the formation of surface structures with hexagonal symmetry.

A. Hexagonal arrays of dots and pits

The weakly nonlinear evolution of a hexagonal surface structure, $h\sim\Sigma_{j=1}^{3}A_j e^{i\mathbf{k}_j\cdot\mathbf{r}}+\text{c.c.}$, where the wave vectors $\mathbf{k}_j$ form an equilateral triangle with the side $k_j=k_c\equiv\sqrt{2}/2$, is usually described by three Ginzburg-Landau–type equations for the complex amplitudes A_j [20,22]. However, in our case the interaction with the Goldstone mode must also be taken into account. Thus, consider $g=g_c-2g_1\epsilon^2$, and

$$h=\epsilon\sum_{j=1}^{3}A_j(\mathbf{R},T)e^{i\mathbf{k}_j\cdot\mathbf{r}}+\epsilon^2B(\mathbf{R},T)+\text{c.c.}+\cdots, \quad (11)$$

where A_j $(j=1,2,3)$ are three complex amplitudes of the unstable modes with wave vectors $\mathbf{k}_j$, respectively, B is the real amplitude of the Goldstone mode, $\mathbf{R}=\epsilon\mathbf{r}$, and $T=\epsilon^2t$. We use the multiple-scale analysis near the bifurcation point to obtain the following system of coupled equations for A_j and B:

$$\partial_T A_j=g_1A_j+2(\mathbf{k}_j\cdot\boldsymbol{\nabla})^2A_j+r_0A_l^*A_n^*+i\sum_{l\neq n\neq j}[A_l^*(r_1\mathbf{k}_l+r_2\mathbf{k}_n)\cdot\boldsymbol{\nabla}A_n^*]-[\lambda_0|A_j|^2+\lambda_1(|A_l|^2+|A_n|^2)]A_j+sA_jB, \quad (12)$$

$$\partial_T B=m\nabla^2B+w\nabla^2(|A_1|^2+|A_2|^2+|A_3|^2), \quad (13)$$

where

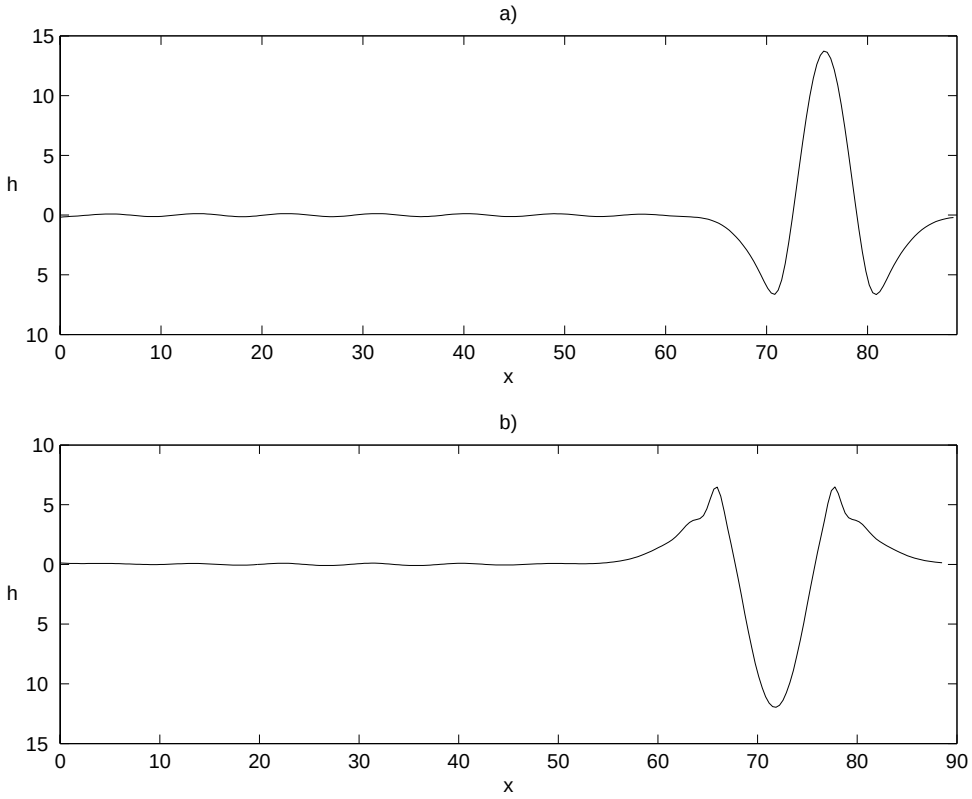

FIG. 6. Numerical solutions of Eq. (5) in 1D at particular moments of time showing intermediate stages of the two types of the blow-up: (a) island type, $g=0.23$, $p=-4.0$, $q=-1.0$, and (b) pit type, $g=0.23$, $p=4.0$, $q=1.0$.

$$\lambda_1=\left(-1+\frac{3}{4}p+q\right)\left(1+\frac{1}{2}p-2q\right), \tag{14}$$

$$r_0=\frac{1}{2}\left(1-\frac{1}{2}p-2q\right), \quad r_1=-p-2r_0,\ r_2=1-2r_0,$$

and other parameters are defined in Eq. (8). The indices j,l,n run from 1 to 3.

Equations (12) and (13) are similar to those derived previously for the interaction between hexagonal Marangoni convection and the long-scale deformational Marangoni instability [18], as well as in several other pattern forming systems with conserved quantities [19]. Note that since a hexagonal pattern occurs via a transcritical bifurcation, Eq. (12) is valid, strictly speaking, only for $r_0=O(\epsilon)$. Otherwise, these equations should be considered as model equations describing weakly nonlinear evolution of a hexagonal pattern (see Ref. [23]). System (12) and (13) has the following stationary solutions:

$$A_j=A_0=\pm\frac{|r_0|+\sqrt{r_0^2+4g_1(\lambda_0+2\lambda_1)}}{2(\lambda_0+2\lambda_1)}, \tag{15}$$

$$B=0,$$

corresponding to a spatially regular pattern of equilateral hexagons, with the signs $\pm$ corresponding to $r_0>0$ and $r_0<0$, respectively. Thus, depending on the sign of the resonant-interaction coefficient r_0, the system can exhibit formation of hexagonal arrays of either mounds (dots) or pits. Dots occur for $r_0>0(A_0>0)$ and pits occur for $r_0<0(A_0<0)$. In both cases, the hexagonal pattern can be stable only for $\lambda_0>0$ and $\lambda_0+2\lambda_1>0$ [22]. Also, in our case, the presence of the Goldstone mode strongly affects the stability of the pattern. A detailed stability analysis of hexagonal patterns in the presence of the Goldstone mode, within the framework of the system (12) and (13), has been recently carried out in the long-wave approximation [19], and it has been shown that if

$$2ws+m(\lambda_0+\lambda_1)<0, \tag{16}$$

a hexagonal pattern is unstable at any supercriticality g_1 [19].

The described stability conditions determine regions in the (q,p) plane where self-organization of hexagonal arrangements of dots or pits can be observed. These regions are shown in Fig. 7. The lines BC and FG correspond to $\lambda_0=0$ and the curves AB, CD, EF, and GH are parts of the hyperbola $\lambda_0+2\lambda_1=0$. Condition (16) holds outside the region bounded by the dashed lines. Inside this region surface structures with hexagonal symmetry can be stable in a certain range of the supercriticality g_1 and the pattern wave number (a ''Busse balloon'') (see Refs. [20,19] and references therein). The lines BK and FL correspond to $r_0=0$ and divide the regions where hexagonal arrays of dots or pits can be observed. Note that the full stability analysis must

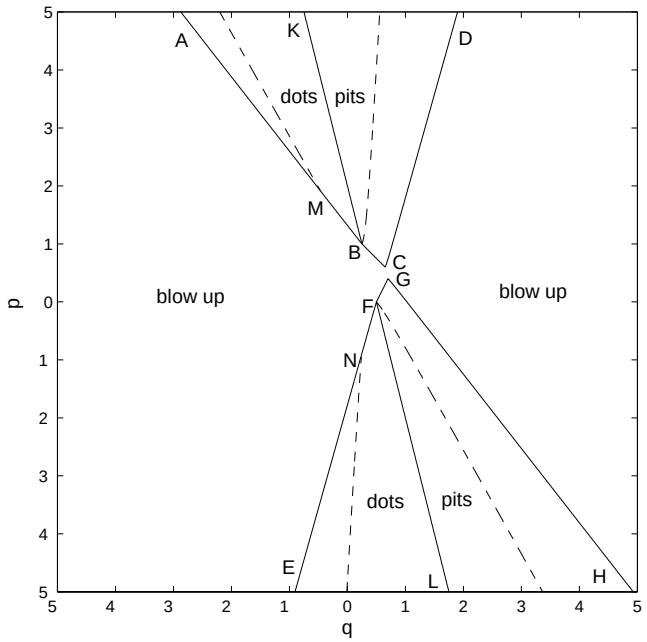

FIG. 7. Regions in (q,p) plane where self-organization of hexagonal arrays of dots or pits can be observed in solutions of Eq. (5) in 2D. The points *B*, *C*, *F*, *G*, *M*, and *N* are (1/4, 1), (13/20, 3/5), (1/2, 0), (7/10, 2/5), $(-0.46,1.91)$, and $(0.24,-0.91)$, respectively.

include the consideration of finite-wavelength instabilities [23] but this is beyond the scope of the present paper.

One can see from Fig. 7 that, unlike the 1+1 case, in the 2+1 system there is an interval $0.4<p<0.6$ [or $|c|<0.1$, see Eq. (6)] in which hexagonal arrays of dots or pits are always subcritical and therefore unstable. Thus, the wetting interaction between the film and the substrate can lead to the self-organization of dots or pits with the almost uniform sizes only if the wetting potential has strong-enough dependence on the surface slope (e.g., sufficient anisotropy), namely, for $|c|>0.1$ or [see Eq. (4)]

$$\left|\frac{\partial\Phi(L,0)}{\partial|\nabla h|^2}\right|>0.4\mu\delta^2. \tag{17}$$

This conclusion is related to the formation of only those regular structures whose characteristic scale is much larger than the critical film thickness.

We have performed numerical simulations of Eq. (5) in 2D by means of a pseudospectral code with periodic boundary conditions. The results of the numerical simulations are shown in Fig. 8. One observes the formation of hexagonal arrays of dots or pits in the parameter regions predicted by the weakly nonlinear analysis. It is interesting that, similar to the 1+1 case, the formation of two types of dots is possible: conelike and caplike [Figs. 8(a,b)]. With the increase of the supercriticality cones transform into caps. Similarly, the formation of two types of pits is observed: ''anticones'' at small supercriticality and ''anticaps'' at larger ones [Figs. 8(c,d)].

B. Wires, rings, and other surface structures

It is known that hexagonal patterns can become unstable with respect to patterns with other symmetries [25,20,22,24]. This instability is determined by the Landau coefficient $\lambda(\phi)$, governing the nonlinear interaction between two modes characterized by two wave vectors $\mathbf{k}_1$ and $\mathbf{k}_2$, $k_1=k_2=k_c$, $\mathbf{k}_1\cdot\mathbf{k}_2=k_c^2\cos\phi$. The Landau coefficient is a function of the angle ϕ between the two wave vectors. Obviously, $\lambda(\phi)$ is defined for $0<\phi<\pi$ and $\lambda(\phi)=\lambda(\pi-\phi)$. Standard multiple-scale analysis of Eq. (5) near the bifurcation threshold $g=g_c$ yields

$$\lambda(\phi)=\left(-\frac{3}{2}+p+2q\right)[\alpha_+(\phi)+\alpha_-(\phi)]+(-1+p)\cos\phi[\alpha_+(\phi)-\alpha_-(\phi)], \tag{18}$$

$$\alpha_\pm(\phi)=\frac{1\pm p\cos\phi-2q}{(\cos\phi\pm 1/2)^2}.$$

Note that the function $\lambda(\phi)$ is singular at $\phi=\pi/3,2\pi/3$ due to the resonant quadratic interaction between these modes, which is responsible for the formation of a hexagonal pattern and is not taken into account in the computation of $\lambda(\phi)$. The Landau (cubic) interaction coefficient in this case is equal to λ_1 in Eq. (14). Note also that $\lambda(0)=\lambda_0+sw/m$, which explains the stability condition (10).

Stability of a hexagonal pattern with respect to patterns with other symmetries was investigated in a number of works (see, e.g., Refs. [25,24,20,22] and references therein). It was shown that, with the increase of the supercriticality, a hexagonal pattern can become unstable with respect to a stripe pattern if $\lambda_1/\lambda_0>1$. The presence of the Goldstone mode, as well as the presence of the quadratic nonlinear terms with the coefficients r_1 and r_2 in Eq. (12) (which characterize the dependence of the resonant quadratic interaction coefficient on the mode wave vectors [23]), can promote the instability [23,19]. In our numerical simulations we have observed the transition from hexagonal arrays of dots or pits to stripe patterns (wires), which occurs with the increase of the supercriticality, g_c-g. These wires are shown in Fig. 9. Transition from dots to wires in epitaxially strained films has been observed in experiments [26].

An interesting surface structure can develop in the parameter regions where $\lambda_0>0,\lambda_1>0$, and $\lambda(\pi/2)<0$. In this case, there is a strong interaction between the modes with orthogonal wave vectors that can lead to a resonant coupling between two systems of hexagons whose basic wave vector sets $(\mathbf{k}_1,\mathbf{k}_2,\mathbf{k}_3)$ and $(\mathbf{k}_4,\mathbf{k}_5,\mathbf{k}_6)$, each forming an equilateral triangle, are mutually orthogonal. This can lead to the formation of a dodecagonal quasiperiodic pattern [27,24]. Our numerical simulation of Eq. (5) shows that such quasiperiodic dodecagonal arrangement of dots can indeed form; it is shown in Fig. 10(a). However, this dodecagonal structure occurs only at the beginning of pattern formation; later in time it either gets replaced by a hexagonal structure or grows further and ultimately blows up. The intermediate stage of the blow-up is shown in Fig. 10(b).

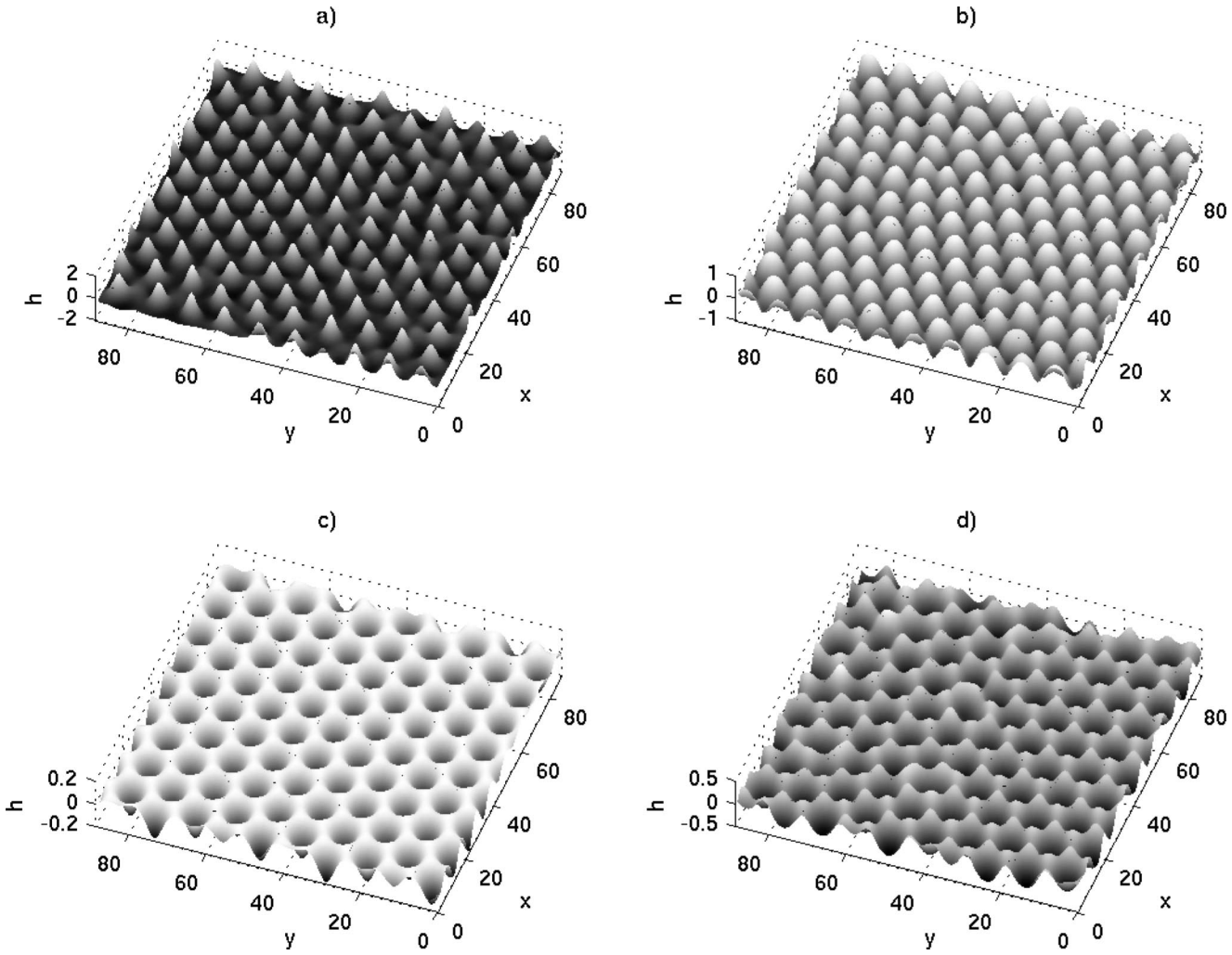

FIG. 8. Numerical solutions of Eq. (5) for various parameter values: (a) hexagonal array of cone-type dots, $p=2.0$, $q=-0.5$, $g=0.2$; (b) hexagonal array of cap-type dots, $p=-4.0$, $q=1.0$, $g=0.01$; (c) hexagonal array of anticone-type pits, $p=-4.0$, $q=2.0$, $g=0.24$; (d) hexagonal array of anticap-type pits, $p=-4.0$, $q=2.0$, $g=0.2$.

In the parameter regions where the hexagonal patterns are subcritical, or unstable according to condition (16), solutions of Eq. (5) blow up in a finite time. Depending on the resonant-interaction coefficient r_0, the blow-up occurs through the formation of high, spatially localized mounds, similar to that shown in Fig. 1, or deep pits. The latter develop into the structures, shown in Fig. 11, that strongly resemble ''quantum rings'' [28] or ''quantum fortresses'' [21] observed in experiments.

V. DISCUSSION AND CONCLUSIONS

We have derived a small-slope nonlinear evolution equation describing the spontaneous formation of quantum dots in an epitaxially strained solid film with wetting interactions between the film and the substrate, near the threshold of the Asaro-Tiller-Grinfeld instability. We have shown that the wetting interaction retards the instability and changes its spectrum so that the instability threshold corresponds to a small but nonzero wave number. This effect causes the formation of spatially regular patterns—hexagonal arrays of dots or pits. Pattern selection and stability are determined by the properties of the wetting potential. We find that unless the wetting potential depends on the slope of the film surface the spatially regular arrays of dots or pits are subcritical and the solutions of the derived equation blow up in a finite time; the weakly nonlinear equation is inapplicable in this case. We have obtained the regions in the plane of dimensionless parameters characterizing the wetting interaction potential where spatially regular arrays of dots or pits can be stable. We have shown that the stability of patterns is strongly affected by the presence of the Goldstone mode associated with the conservation of mass.

Spontaneous formation of hexagonal arrays of quantum dots has been observed in several processes: ion sputtering [29], self-assembling of Ag monolayers on Ru [30], Pb on Cu [31], and Ge on Si(111)-(7×7) [32], as well as in the multilayer growth of superlattices [33]. Currently, we are not aware of any observation of a spontaneous self-organization of hexagonal arrays of dots or pits resulting from the ATG instability of epitaxially strained solid films. In fact, this may be difficult to observe since hexagonal structure is formed

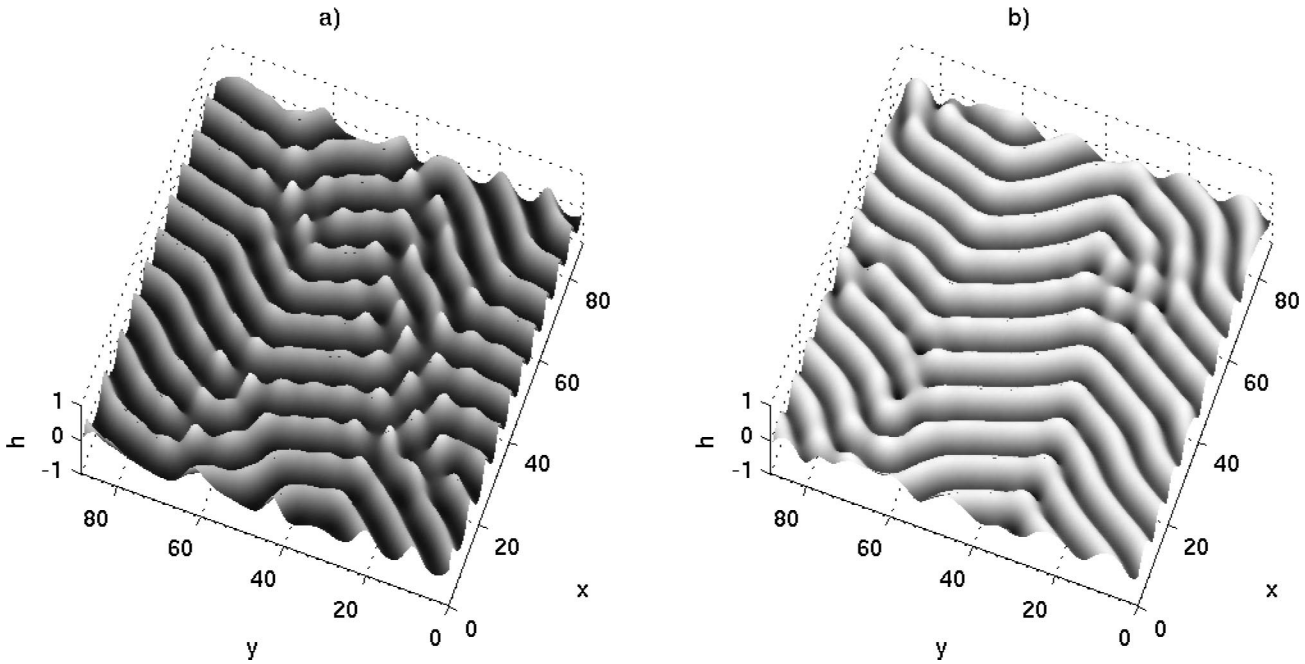

FIG. 9. Formation of ''wire'' patterns via transition from (a) dots, $p=4.0$, $q=-1.0$, $g=0.1$; (b) pits, $p=-4.0$, $q=2.0$, $g=0.1$.

near the instability threshold and it becomes unstable with the increase of the supercriticality. A very precise tuning of parameters would be required in order to achieve near-threshold conditions. However, it is important that our analysis shows a principal possibility of such self-organization of quantum dots in Stranski-Krastanow growth.

Our model also describes interesting phenomena such as a transition from quantum dots to quantum wires [26] and the formation of quantum rings or isotropic quantum fortresses [21,28]. Although the latter appears in the present model as a transitional stage of the blow-up solution, the mechanism of the ring formation—specific properties of the wetting interaction between the film and the substrate—may well be captured. Of course, the derived weakly nonlinear model cannot described the full dynamics of this process.

Note that the present model is derived in the small-slope approximation that holds in the presence of the wetting interaction only if the wetting potential Φ satisfies conditions (4). These conditions put strong restrictions on the type of the potential Φ for which the approximation can be valid.

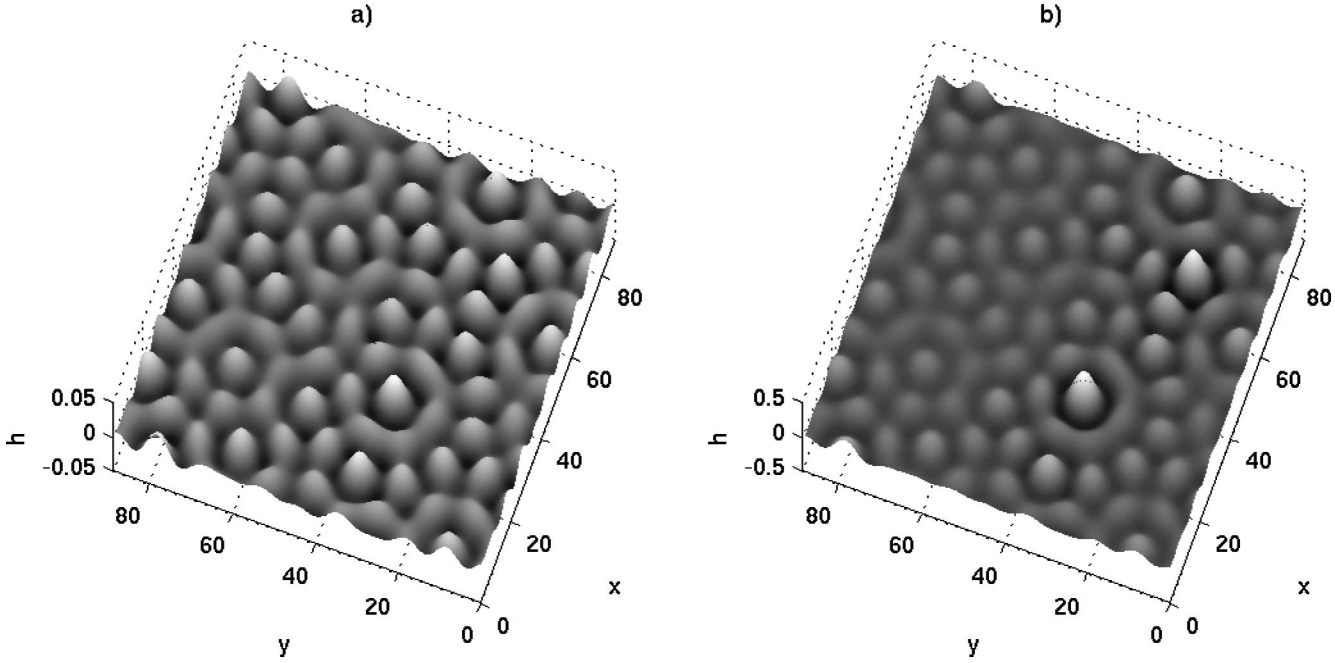

FIG. 10. Formation of a quasiperiodic array of dots with dodecagonal symmetry, $p=-3.0$, $q=-0.1$, $g=0.249$. (a) Initial stage of formation; (b) intermediate stage of the blow-up.

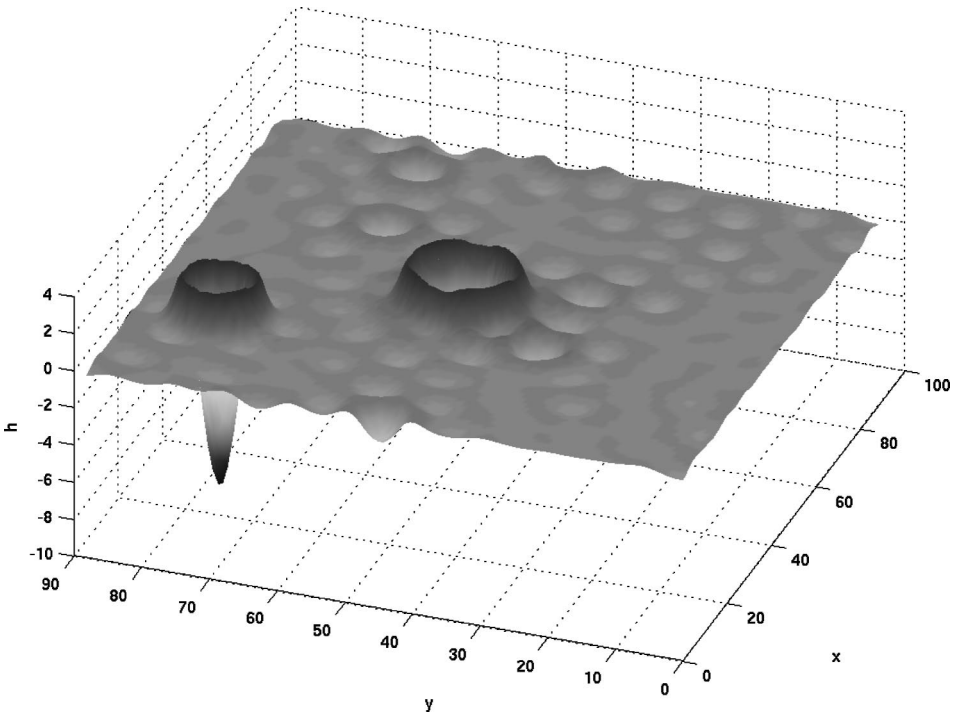

FIG. 11. Intermediate stage of the blow-up solution of Eq. (5) in the form of a ''quantum ring''; $p=2.0$, $q=1.0$, $g=0.2$.

Probably the most important restriction is the strong dependence of the wetting potential on the surface slope. For example, in the case of the ''two-layer'' model, in which the wetting interaction is defined by a thickness-dependent surface tension $\gamma(h)$, so that $\Phi=(d\gamma/dh)/(1+|\nabla h|^2)^{1/2}$ [12], conditions (4) would imply $L|\partial\Phi/\partial h|\ll\Phi, L^2|\partial^2\Phi/\partial h^2|\ll\Phi$, and $|\partial\Phi/\partial h|\ll L|\partial^2\Phi/\partial h^2|$. These inequalities can hold, for instance, near the extremum of the function $\Phi(h)$, provided the function is not monotonic. At the same time, a sufficiently strong dependence of the wetting potential on the surface slope can be expected in the presence of large anisotropy. Note also that if one assumes that the wetting potential can depend on the curvature of the film surface, this can change the sign of the nonlinear term $\nabla^2[h\nabla^2 h]$ in Eq. (5). In this case all the described results are valid after the transformation $p\to -p, q\to -q, h\to -h$.

To conclude, we have chosen the small-slope approximation and the case of a rigid substrate as the first step in understanding possible effects of the wetting interactions on the formation of quantum dots resulting from the ATG instability of epitaxially strained solid films. Since the main effect—the change of the instability spectrum from the long wave ($k_c=0$) to the short wave ($k_c\neq 0$)—depends neither on the rigid-substrate assumption nor on the small-slope approximation, one can investigate, by means of the weakly nonlinear analysis, pattern formation in more general cases in which these assumptions are relaxed.

ACKNOWLEDGMENTS

This work was supported by the National Science Foundation Grant No. 0102794 and by the Binational US-Israel Science Foundation Grant No. 9800086.

[1] R.J. Asaro and W.A. Tiller, Metall. Trans. **3**, 1789 (1972); M.Ya. Grinfeld, Sov. Phys. Dokl. **31**, 831 (1986).
[2] D.J. Srolovitz, Acta Metall. **17**, 621 (1989); B.J. Spencer, P.W. Voorhees, and S.H. Davis, Phys. Rev. Lett. **67**, 3696 (1991).
[3] F.M. Ross, J. Tersoff, and R.M. Tromp, Phys. Rev. Lett. **80**, 984 (1998).
[4] K. Alchalabi, D. Zimin, G. Kostorz, and H. Zogg, Phys. Rev. Lett. **90**, 026104 (2003).
[5] V.A. Shchukin and D. Bimberg, Rev. Mod. Phys. **71**, 1125 (1999).
[6] Y.W. Zhang, Phys. Rev. B **61**, 10 388 (2000); Y.W. Zhang and A.F. Bower, Appl. Phys. Lett. **78**, 2706 (2001).
[7] P. Liu, Y.W. Zhang, and C. Lu, Phys. Rev. B **68**, 035402 (2003).
[8] B.J. Spencer, S.H. Davis, and P.W. Voorhees, Phys. Rev. B **47**, 9760 (1993).
[9] Y. Xiang and Weinan E, J. Appl. Phys. **91**, 9414 (2002).
[10] W.H. Yang and D.J. Srolovitz, Phys. Rev. Lett. **71**, 1593 (1993); B.J. Spencer and D.I. Meiron, Acta Metall. Mater. **42**, 3629 (1994).
[11] H.R. Eisenberg and D. Kandel, Phys. Rev. Lett. **85**, 1286 (2000).
[12] B.J. Spencer, Phys. Rev. B **59**, 2011 (1999).
[13] M. Ortiz, E.A. Repetto, and H. Si, J. Mech. Phys. Solids **47**, 697 (1999).
[14] H.R. Eisenberg and D. Kandel, Phys. Rev. B **66**, 155429 (2002).
[15] M.I. Tribelskii, Usp. Fiz. Nauk **167**, 167 (1997).

[16] P.C. Matthews and S.M. Cox, Nonlinearity **13**, 1293 (2000).
[17] A.A. Golovin, A.A. Nepomnyashchy, and L.M. Pismen, Phys. Fluids **6**, 34 (1994).
[18] A.A. Golovin, A.A. Nepomnyashchy, and L.M. Pismen, J. Fluid Mech. **341**, 317 (1997).
[19] S.M. Cox and P.C. Matthews, Physica D **175**, 196 (2003).
[20] M.C. Cross and P.C. Hohenberg, Rev. Mod. Phys. **65**, 851 (1993).
[21] J.L. Gray, R. Hull, and J.A. Floro, Appl. Phys. Lett. **81**, 2445 (2002).
[22] D. Walgraef, *Spatio-Temporal Pattern Formation* (Springer, New York, 1997).
[23] A.E. Nuz, A.A. Nepomnyashchy, A.A. Golovin, A. Hari, and L.M. Pismen Physica D **135**, 233 (2000).
[24] A.A. Golovin, A.A. Nepomnyashchy, and L.M. Pismen, Physica D **81**, 117 (1995).
[25] B.A. Malomed and M.I. Tribelsky, Zh. Eksp. Teor. Fiz. **92**, 539 (1987) [Sov. Phys. JETP **65**, 305 (1987)].
[26] T. Mano, R. Nötzel, G.J. Hamhuis, T.J. Eijkemans, and J.H. Wolter, J. Appl. Phys. **92**, 4043 (2002).
[27] B.A. Malomed, A.A. Nepomnyashchy, and M.I. Tribelsky, Zh. Eksp. Teor. Fiz. **96**, 684 (1989) [Sov. Phys. JETP **69**, 388 (1989)].
[28] D. Granados and J.M. Garcia, Appl. Phys. Lett. **82**, 2401 (2003).
[29] S. Facsko, T. Bobek, T. Dekorsy, and H. Kurz, Phys. Status Solidi B **224**, 537 (2001).
[30] K. Pohl, M.C. Bartelt, J. de la Figuera, N.C. Bartelt, J. Hrbek, and R.Q. Hwang, Nature (London) **397**, 238 (1999).
[31] R. Plass, J.A. Last, N.C. Bartelt, and G.L. Kellog, Nature (London) **412**, 875 (2001).
[32] Y.P. Zhang, L. Yan, S.S. Xie, S.J. Pang, and H.-J. Gao, Appl. Phys. Lett. **79**, 3317 (2001).
[33] M. Pinczolits, G. Springholz, and G. Bauer, Phys. Rev. B **60**, 11 524 (1999).